ATTRIBUTION OF THE 2017 NORTHERN HIGH PLAINS DROUGHT

Hailan Wang, Siegfried D. Schubert, Randal D. Koster, and Yehui Chang

The 2017 northern High Plains precipitation deficits were largely the result of internal atmospheric variability. Global warming may have exacerbated the dry condition by producing surface warming and increasing the probability of heat waves there.

INTRODUCTION. The northern High Plains, particularly much of Montana and the Dakotas, had extreme to exceptional drought conditions develop during the summer of 2017. When the months of May, June, and July are combined, the year 2017 received 60% of normal precipitation and is ranked as the second driest (only after 1936) of the period 1901–2017 (Fig. 1a; see also Fig. ES1a in the online supplemental material). It also had anomalously warm temperatures relative to the 1901–2017 record (Figs. 1b and ES1b). The exceptional dryness combined with the unusual heat over central and eastern Montana resulted in a rapidly declining Palmer Severity Drought Index, which, although of short duration, reached extreme drought levels comparable to those of historical droughts (e.g., during the 1930s). The occurrence of the drought over Montana and the Dakotas, an important spring wheat–growing region in the country, during the crop growing season caused agricultural losses of $2.5 billion and contributed to one of Montana's worst wildfire seasons on record (NOAA/NCEI 2018).

AFFILIATIONS: Wang—Science Systems and Applications, Inc., Lanham, Maryland; Schubert—Global Modeling and Assimilation Office, NASA Goddard Space Flight Center, Greenbelt, and Science Systems and Applications, Inc., Lanham, Maryland; Koster— Global Modeling and Assimilation Office, NASA Goddard Space Flight Center, Greenbelt, Maryland; Chang—Global Modeling and Assimilation Office, NASA Goddard Space Flight Center, Greenbelt, and Morgan State University, Baltimore, Maryland

CORRESPONDING AUTHOR: Dr. Hailan Wang, hailan.wang-1@nasa.gov

DOI:10.1175/BAMS-D-18-0115.1

A supplement to this article is available online (10.1175/BAMS-D-18-0115.2)

This study investigates the causes of the 2017 northern High Plains drought, particularly the roles of the 2017 sea surface temperature (SST) anomalies and atmospheric internal variability. It also assesses the impact of the post-1901 long-term warming trend on the frequency of drought occurrence in the area.

DATA AND METHODS. This study makes use of various observational datasets, including the NOAA Extended Reconstructed SST (ERSST) version 5 (Huang et al. 2017), the Global Precipitation Climatology Project (GPCP) precipitation (Adler et al. 2003), and the Global Precipitation Climatology Centre (GPCC) land precipitation (Schneider et al. 2014). Data from the NASA Modern-Era Retrospective Analysis for Research and Applications, version 2 (MERRA-2; Gelaro et al. 2017) are used as well.

The study also utilizes two sets of Atmospheric Model Intercomparison Project (AMIP) simulations performed with the NASA Goddard Earth Observing System Model, version 5 (GEOS-5) atmospheric general circulation model (AGCM) (Rienecker et al. 2008; Molod et al. 2012), forced with observed monthly SST, sea ice, and time-varying greenhouse gases (Schubert et al. 2014). The first set is used to investigate the impacts of the 2017 SST anomalies and atmospheric internal variability on the drought event in the context of current climate; here, a GEOS-5 (tag: Ganymed 4.0) AMIP simulation covering 1980–2014 provided a climatology, and a 90-member ensemble of AMIP simulations performed for 2017 provided a robust estimate of model atmospheric internal variability during that year. These AMIP runs employed a tendency bias correction to the basic state variables (estimated from the time-mean MERRA-2 analysis increments) that removes much of the model bias in the mean climate and its variability (Wang et al. 2018). The second set of AMIP simulations consists of 12 archived long-

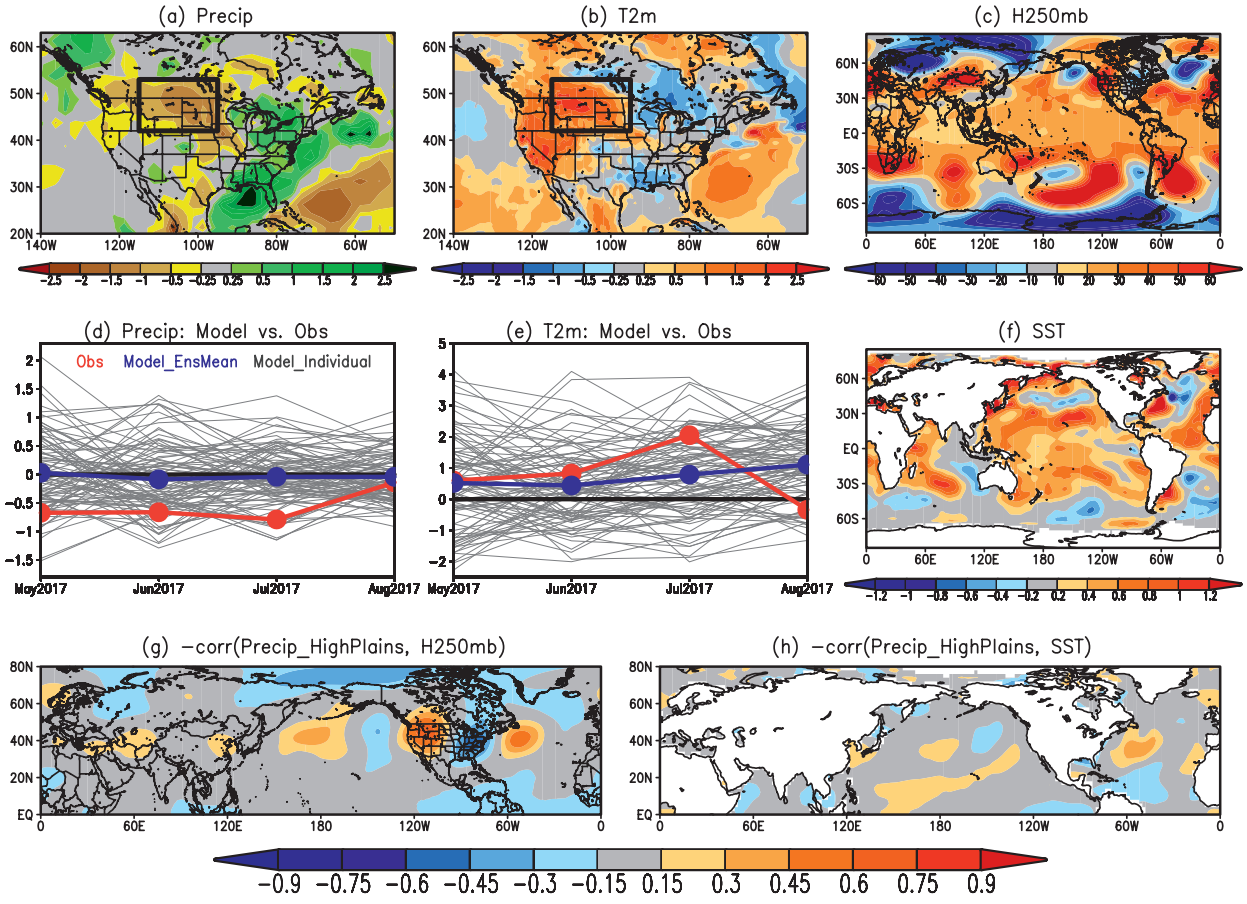

Fig. 1. The observed May–July 2017 anomalies in (a) precipitation from GPCP (mm day^{-1}), (b) surface air temperature anomalies (K) from MERRA-2, and (c) 250-mb geopotential height (m) from MERRA-2. (d) The comparison between observations (GPCP), the 90 GEOS-5 AMIP members, and their ensemble mean for monthly precipitation anomalies (mm day^{-1}) averaged over the 2017 drought region (245°–265°E, 42°–53°N) for May–August 2017. (e) As in (d), but for surface air temperature (K). (f) As in (a), but for NOAA SST (unit: K). (g) The temporal correlation between GPCP precipitation averaged over the 2017 drought region and MERRA-2 250-mb geopotential height for May–July averages for 1980–2017; (h) as in (g), but for NOAA SST. The above anomalies are obtained as deviations from their climatology over the period 1980–2014. The 2017 drought region is indicated using a black box in (a) and (b).

term simulations (1901–2014) performed with an earlier version of the GEOS-5 AGCM (tag: Fortuna 2.4) (Schubert et al. 2014); it is used to assess the effects of historical warming. The dependence of the attribution analysis on climatologies used and the model dependence of our assessments are examined by also considering long-term NCAR CAM5 AMIP simulations (1901–2017; 40 members).[1] Since the precipitation deficit and surface warming anomalies in the northern High Plains mainly occurred during May–July 2017, our analyses focus on the average of these three months.

RESULTS. Figure 1 examines the 2017 northern High Plains drought relative to the 1980–2014 climatology. The observed May–July averaged precipitation deficits occurred over the northern Plains and southern Canadian prairies (Fig. 1a). Meanwhile, much of the western half of the United States experienced warmer-than-normal temperatures, with peak warming over Montana, the Dakotas, and the southwestern United States (Fig. 1b). The accompanying geopotential height anomalies in the upper troposphere consisted of widespread warming in the tropics and much of the midlatitudes, a reflection of global SST warming trends during recent decades (e.g., Schubert et al. 2014), as well as a zonal wave train that spans the North Pacific and North America, with an anomalous barotropic high centered over the northwestern United States (Fig. 1c). The high anomaly, which

[1] The long-term NCAR CAM5 AMIP simulations are produced by the NOAA ESRL Attribution and Predictability Assessments Team and are made available at the NOAA/ESRL/PSD Climate Data Repository (www.esrl.noaa.gov/psd/repository/alias/facts).

persisted throughout much of May–July 2017 (not shown), contributed to the local surface warming by suppressing the formation of local convection and clouds and leading to increased solar radiation at the surface. Meanwhile, the northerly anomaly at its east flank in the lower troposphere weakened the Great Plains low-level jet (LLJ) and inhibited northward atmospheric moisture transport by the jet, leading to precipitation deficits in the northern High Plains.

To investigate the physical processes for the 2017 drought event, we compared anomalies from the first set of GEOS-5 AMIP simulations with observations (Figs. 1d,e). Here the model ensemble average highlights the SST-forced signal, whereas the spread among the ensemble members reflects the unforced variability generated by processes internal to the atmosphere. The observed SST anomalies show warming over much of the tropical and subtropical oceans (Fig. 1f). When forced with these SST anomalies, the ensemble mean of the GEOS-5 AGCM simulations shows little change in precipitation but a notable surface warming in the northern High Plains. The observed anomalies fall within the fairly large model ensemble spread, with the observed precipitation anomalies falling near the dry edge of the spread. Only three ensemble members (out of 90) show persistent dry and warm responses similar to the observations. These results suggest that the 2017 warm SST anomalies encouraged surface warming in the northern High Plains, while atmospheric internal variability explains much of the precipitation deficits. A parallel analysis using the CAM5 AMIP simulations (1901–2017) shows that the above conclusion is not changed when viewed in the context of the century long (1901–2014) climate (cf. Figs. 1d,e with Figs. ES1c–f); furthermore, it appears that much of the 2017 SST-forced surface warming in the northern High Plains is a response to the long-term SST warming trend (see the online supplemental information). Figure 1g shows that the year-to-year variation of summertime precipitation in the northern High Plains is typically associated with a zonal wave train (of roughly wavenumber 5) in the NH midlatitudes; its connection to SST is weak overall (Fig. 1h). Such a wave train resembles the leading patterns of upper-level circulation variability within the jet waveguide during boreal summer (Ding and Wang 2005; Schubert et al. 2011). The nature of the drought-inducing atmospheric internal variability is yet unclear and needs further research.

In our second analysis, we investigate the effect of historical warming on the occurrence of extreme dry events in the northern High Plains by comparing two time periods from the long-term GEOS-5 AMIP simulations: 1901–70 and 1980–2014, with the latter period coinciding with the start of a period of enhanced global warming. The May–July mean SST differences between the two periods (Fig. 2a) reflects the long-term warming trend over the twentieth century, as evidenced by its resemblance to the SST warming trend pattern that is obtained as the leading rotated empirical orthogonal function (REOF) of annual mean SST over 1901–2004 (Schubert et al. 2009). Most of the effects of decadal to multidecadal oscillations (e.g., the Pacific decadal oscillation and Atlantic multidecadal oscillation) are thus averaged out in the two periods. Relative to the early period, the ensemble mean upper-level geopotential height in the latter period (Fig. 2b) increases nearly everywhere, with local maxima occurring over the northwestern United States and the Bering Sea, presumably forced by the long-term SST changes (Fig. 2a). In fact, such atmospheric circulation changes resemble the responses of this model and four other AGCMs participating in the U.S. CLIVAR drought working group (Schubert et al. 2009) to the above-mentioned SST warming trend pattern (not shown), suggesting that the circulation changes in Fig. 2b are a robust dynamical response to the warming trend pattern.

We investigate the effects of historical global warming on the occurrence of drought extremes in the northern High Plains by comparing the probability density functions (PDFs) of drought-related variables in the two periods. The precipitation PDFs in the northern High Plains for the two periods are very similar (Fig. 2c), consistent with indications from GPCC observations (not shown). There are, however, clear indications of an increased probability of warmer surface air temperature in the recent period (Fig. 2d), which leads to a modest increase in the risk for drier soil (Fig. 2e). The AMIP simulations thus suggest that agricultural droughts (soil moisture deficits) are more probable during recent times. Evapotranspiration shows a slight net decrease (not shown), a reflection of the slight decrease in precipitation. There are also clear indications of an increased probability of a moister atmosphere over the central United States (Fig. 2f) and increased eddy height anomalies over the northwestern United States (Fig. 2g). While the moister atmosphere tends to increase atmospheric moisture transport to the northern High Plains and thus precipitation there, the increased eddy height anomalies tend to reduce this precipitation by inducing subsidence in the northern High Plains as well as by weakening the Great Plains LLJ. In other words, the modest

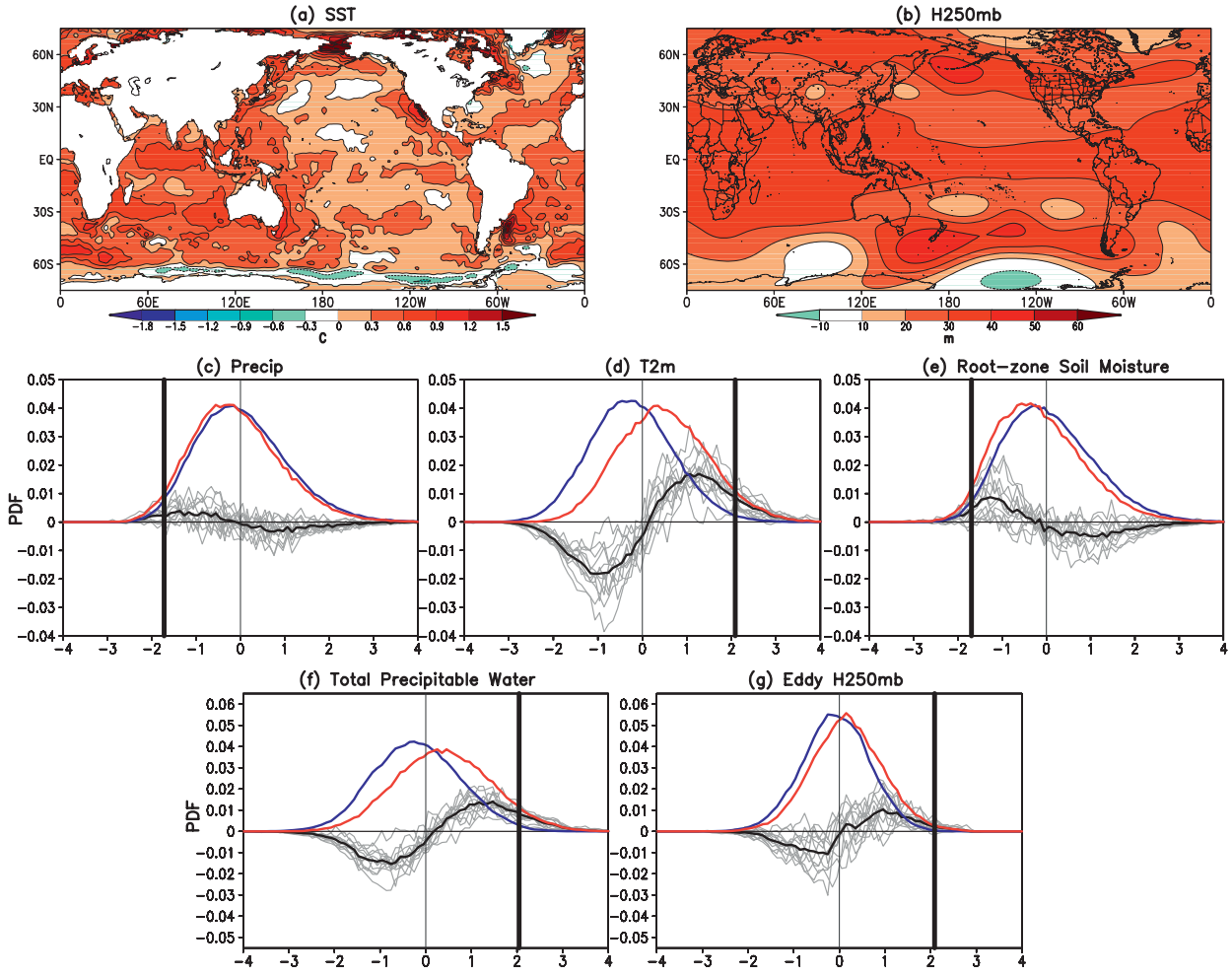

Fig. 2. (a) The observed climatology difference of May–July SST between the periods 1901–70 and 1980–2014. (b) As in (a), but for the 250-mb geopotential height in the GEOS-5 AMIP ensemble mean simulation. (c) The PDF of precipitation over the 2017 drought region (245°–265°E; 42°–53°N) for the periods 1901–70 (blue) and 1980–2014 (red) using the 12 GEOS-5 AMIP simulations combined, the PDF difference between the two time periods using the 12 AMIP simulations combined (black), and each of the 12 AMIP simulations (gray). (d),(e) As in (c), but respectively for surface air temperature and root-zone soil moisture (moisture in the top meter of soil, as determined from soil moisture prognostic states in the GEOS-5 land surface model). (f),(g) As in (c), but respectively for total column water vapor over the central United States (245°–265°E; 30°–45°N) and the 250-mb zonally asymmetric geopotential height over the northwestern United States (232°–257°E, 35°–52°N). The critical values of 2.5% associated with dry conditions based on the distribution over 1901–2014 are shown using thick black vertical lines. [Note that the PDF analysis in (c)–(g) uses data at all grid points in the selected domains. Anomalies used in the PDF analysis are normalized deviations from the climatology over the period 1901–2014.]

change in the precipitation PDF (Fig. 2c) appears to reflect counteracting impacts of the thermodynamic and dynamical processes. A parallel analysis using the CAM5 simulations (Fig. ES2) produces results similar to those based on the GEOS-5 model (Fig. 2), supporting that our findings are not model dependent. We also emphasize that the impact of dynamical processes examined here reflects the model's response to the observed SST changes that occurred during the period of 1901–2014. As such, the dynamical impact may be different in models (e.g., CMIP5 historical simulations) that simulate mean SST changes different from the observed.

CONCLUSIONS. The 2017 northern High Plains drought and associated heat waves were induced in part by a positive height anomaly that persisted over the northwestern United States and the northern High Plains throughout much of May–July 2017. Our model results show that while the observed 2017 SST anomalies provided a predilection for drought by inducing surface warming, internal atmospheric vari-

ability accounts for the extreme precipitation deficits.

An assessment of the role of historical global warming shows no appreciable increase in the risk of precipitation deficits but an increased risk of heat waves in the northern High Plains. In fact, a substantial fraction of the 2017 SST-forced surface warming appears to be a response to the global warming signal. The small change in the probability of precipitation deficits over the historical period appears to reflect counteracting effects of thermodynamic processes (increased atmospheric moisture over the United States) and dynamical processes (increased eddy height over the northwestern United States). The increased risk for heat waves may have increased the likelihood of agricultural (soil moisture) drought in the region, and contributed to exacerbating the 2017 drought.

ACKNOWLEDGMENTS. This work has been supported by the NOAA Climate Program Office Modeling, Analysis, Prediction, and Projections (MAPP) program and the NASA Modeling, Analysis and Prediction (MAP) program. We thank Peter Stott, Martin Hoerling, and two anonymous reviewers for their constructive comments and suggestions, which have greatly improved the paper.

REFERENCES

Adler, R. F., and Coauthors, 2003: The version-2 Global Precipitation Climatology Project (GPCP) monthly precipitation analysis (1979–present). *J. Hydrometeor.*, **4**, 1147–1167, https://doi.org/10.1175/1525-7541(2003)004<1147:TVGPCP>2.0.CO;2.

Ding, Q., and B. Wang, 2005: Circumglobal teleconnection in the Northern Hemisphere summer. *J. Climate*, **18**, 3483–3505, https://doi.org/10.1175/JCLI3473.1.

Gelaro, R., and Coauthors, 2017: The Modern-Era Retrospective Analysis for Research and Applications, version 2 (MERRA-2). *J. Climate*, **30**, 5419–5454, https://doi.org/10.1175/JCLI-D-16-0758.1.

Huang, B., and Coauthors, 2017: Extended Reconstructed Sea Surface Temperature version 5 (ERSSTv5), Upgrades, validations, and intercomparisons. *J. Climate*, 30, 8179–8205, https://doi.org/10.1175/JCLI-D-16-0836.1.

Molod, A., L. Takacs, M. Suarez, J. Bacmeister, I.-S. Song, and A. Eichmann, 2012. The GEOS-5 atmospheric general circulation model: Mean climate and development from MERRA to Fortuna. NASA Technical Report Series on Global Modeling and Data Assimilation, NASA TM-2012-104606, Vol. 28, 117 pp.

NOAA/NCEI, 2018: Billion-dollar weather and climate disasters. NOAA National Centers for Environmental Information, accessed xxxx, www.ncdc.noaa.gov/billions/.

Rienecker, M. M., and Coauthors, 2008: The GEOS-5 data assimilation system—Documentation of versions 5.0.1, 5.1.0, and 5.2.0. NASA Tech. Rep. Series on Global Modeling and Data Assimilation, NASA/TM-2007-104606, Vol. 27, 95 pp.

Schneider, U., A. Becker, P. Finger, A. Meyer-Christoffer, M. Ziese, and B. Rudolf, 2014: GPCC's new land surface precipitation climatology based on quality-controlled in situ data and its role in quantifying the global water cycle. *Theor. Appl. Climatol.*, **115**, 15–40, https://doi.org/10.1007/s00704-013-0860-x.

Schubert, S., and Coauthors, 2009: A U.S. CLIVAR project to assess and compare the responses of global climate models to drought-related SST forcing patterns: Overview and results. *J. Climate*, **22**, 5251–5272, https://doi.org/10.1175/2009JCLI3060.1.

——, H. Wang, and M. Suarez, 2011: Warm season subseasonal variability and climate extremes in the Northern Hemisphere: The role of stationary Rossby waves. *J. Climate*, **24**, 4773–4792, https://doi.org/10.1175/JCLI-D-10-05035.1.

——, ——, R. Koster, M. Suarez, and P. Groisman, 2014: Northern Eurasian heat waves and droughts. *J. Climate*, **27**, 3169–3207, https://doi.org/10.1175/JCLI-D-13-00360.1.

Wang, H., S. D. Schubert, Y. Chang, and R. D. Koster, 2018: Subseasonal prediction of warm season drought in North America. *42nd NOAA Climate Diagnostics and Prediction Workshop*, Norman, OK, National Weather Service, www.cpc.ncep.noaa.gov/products/outreach/CDPW42/11-Wang.pdf.